Anal Bioanal Chem (2008) 391:2119–2125
DOI 10.1007/s00216-008-2162-1

ORIGINAL PAPER

Endocytosis of a single mesoporous silica nanoparticle into a human lung cancer cell observed by differential interference contrast microscopy

Wei Sun · Ning Fang · Brian G. Trewyn · Makoto Tsunoda · Igor I. Slowing · Victor S. Y. Lin · Edward S. Yeung

Received: 7 March 2008 / Revised: 24 April 2008 / Accepted: 25 April 2008 / Published online: 17 May 2008

Abstract The unique structural features of mesoporous silica nanoparticles (MSN) have made them very useful in biological applications, such as gene therapy and drug delivery. Flow cytometry, confocal microscopy, and electron microscopy have been used for observing the endocytosis of MSN. However, flow cytometry cannot directly observe the process of endocytosis. Confocal microscopy requires fluorescence labeling of the cells. Electron microscopy can only utilize fixed cells. In the present work, we demonstrate for the first time that differential interference contrast (DIC) microscopy can be used to observe the entire endocytosis process of MSN into living human lung cancer cells (A549) without fluorescence staining. There are three physical observables that characterize the locations of MSN and the stages of the endocytosis process: motion, shape, and vertical position. When it was outside the cell, the MSN underwent significant Brownian motion in the cell growth medium. When it was trapped on the cell membrane, the motion of the MSN was greatly limited. After the MSN had entered the cell, it resumed motion at a much slower speed because the cytoplasm is more viscous than the cell growth medium and the cellular cytoskeleton networks act as obstacles. Moreover, there were shape changes around the MSN due to the formation of a vesicle after the MSN had been trapped on the cell membrane and prior to entry into the cell. Finally, by coupling a motorized vertical stage to the DIC microscope, we recorded the location of the MSN in three dimensions. Such accurate 3D particle tracking ability in living cells is essential for studies of selectively targeted drug delivery based on endocytosis.

Keywords Endocytosis · Mesoporous silica nanoparticle · Differential interference · Brownian motion

W. Sun · N. Fang · B. G. Trewyn · M. Tsunoda · I. I. Slowing · V. S. Y. Lin · E. S. Yeung (✉)
Ames Laboratory-USDOE and Department of Chemistry,
Iowa State University,
Ames, IA 50011, USA
e-mail: yeung@ameslab.gov

Introduction

Mesoporous silica nanoparticle (MSN) materials have many unique features, such as chemical stability, tunable pore diameter (2–30 nm), narrow pore size distribution, and high surface area (more than 700 m^2 g^{-1}). Moreover, the pores inside MSNs are independent parallel channels that can be capped and opened by controllable chemical stimulation [1], photo stimulation [2], or pH stimulation [3]. The digestion of guest molecules can be avoided because guest molecules are protected against enzymes before they reach their destinations. Furthermore, compared with viral vectors, MSNs cause fewer pathogenic risks [4] and compared with polymer nanoparticles, MSNs are more resistant to organic solvents [5]. It has already been demonstrated that MSNs are biocompatible and can be endocytosed by animal and plant cells [6, 7].

Because of these unique features, MSNs have been used as carriers in a controlled-release delivery system to transfer cell membrane impermeable molecules [8]. In order to increase cell recognition and selective endocytosis of MSNs, it is of great importance to observe and understand the entire process of endocytosis of MSNs. Flow cytometry, confocal microscopy, and electron microscopy have been employed previously for this purpose [8–11]. Flow cytometry can be used to study the efficiency of endocytosis by converting the measured fluorescence intensity into the

number of MSNs present inside the cell, but it cannot provide information during the process of endocytosis or show the distribution of MSNs inside the cell. Confocal microscopy can be used for live-cell imaging, but the cells need to be stained with fluorescent dyes. In electron microscopy, more detailed information can be extracted, including the distribution of MSNs; however, because the cells are fixed and dead, this technique cannot track the continuous movement of MSNs inside living cells directly.

In the present study, various modes of optical microscopy were tested for nonintrusive, continuous tracking of sub-diffraction-limited MSNs during the entire endocytosis process in living cells. The application of bright-field microscopy is limited because there is too little contrast between MSNs, the cells, and the surrounding medium. The contrast can be greatly improved by using phase-contrast microscopy, dark-field microscopy, or differential interference contrast (DIC) microscopy. These three techniques have been compared previously for horizontal resolving power and vertical sectioning ability [12]. In phase-contrast microscopy, halos were always seen around the edges of the cell membrane and intracellular organelles, blurring some details. In dark-field microscopy, which mainly depends on light scattering of objects, we noticed that inside eukaryotic cells, especially around cell nuclei, the scattering light was too strong to resolve particles of sub-200-nm diameter. In addition, dark-field microscopy requires strong incident light, which is not suitable for long-time observation of living cells.

DIC microscopy not only increases the contrast between cells and the surrounding medium, but also has some other advantages over phase-contrast and dark-field microscopy [13]. DIC microscopy does not have the "halo" edge effect, and it does not cause much scattering inside the cell. DIC microscopy makes full use of the numerical aperture of the system and has a shallow depth of focus, leading to a much better vertical resolution and thus good optical sectioning. Moreover, DIC microscopy utilizes the interference of light instead of the opacity of the specimen; it can resolve objects which are smaller than the theoretical resolution limit of optical microscopy. The MSN of around 100 nm in diameter used in our experiment is one example.

DIC microscopy is useful for particle uptake studies in living cells, and it has already been demonstrated [14]. Here we further the application of DIC microscopy for single-particle tracking in living cells. In our experiment, we used DIC microscopy to record the entire process of endocytosis of a single MSN by a living human lung cancer cell (A549) without staining the cell. Unlike in electron microscopy, the cells were alive during the entire recording period and the endocytosis process was tracked continuously from start to finish. Three physical observables—motion speed, shape, and vertical position—were used to characterize the locations of the MSN (inside/outside the cell or on the cell membrane) throughout the many stages of the endocytosis process.

Experimental

Synthesis of fluorescein isothiocyanate labeled and tri (ethylene glycol) organic linker modified MSNs

Tetraethyl orthosilicate (TEOS) was purchased from Gelest (Philadelphia, PA, USA). Fluorescein isothiocyanate (FTIC) isomer I, anhydrous dimethyl sulfoxide, 3-aminopropyl-trimethoxysilane (APTMS), and cetyltrimethylammonium bromide were purchased from Sigma-Aldrich (St. Louis, MO, USA). All chemicals were used as received. FITC-labeled MSNs were prepared by reacting 5.0 mg (1.284 mmol) of FITC with 40 μl (1.146 mmol) of APTMS in anhydrous dimethyl sulfoxide under an inert atmosphere for 2 h, and then co-condensing the resulting product with 5.0 ml (32.5 mmol) TEOS by the hydrothermal method previously reported [11]. To a mixture of 1.0 g (2.75 mmol) cetyltrimethylammonium bromide, 480 ml water and 3.5 ml 2 M sodium hydroxide, heated at 80 °C, under vigorous stirring, the TEOS and the product of the FITC and APTMS reaction were added dropwise. The reaction mixture was maintained at 80 °C for 2 h, after which the resulting orange solid was filtered, washed thoroughly with water and methanol, and dried under vacuum at 80 °C for 20 h. The synthesis of the organic ligand was achieved by modifying a procedure previously reported [15]. Specifically the synthesis of 1-[2-(2-bromoethoxy)ethoxy]-2-methoxy-ethane was followed directly, then this molecule was attached to APTMS via an SN^2 reaction in refluxing ethanol overnight. This crude product was directly grafted to as-synthesized FITC–MSNs (still containing a surfactant template). Once grafted, the surfactant template was removed via our previously published method [16]. The average diameter of these FITC-labeled spherical MSNs measured by transmission electron microscopy was around 100 nm (Fig. 1).

Cell culture

Human lung cancer cells (A549) were purchased from American Type Culture Collection (ATCC, Baltimore, USA; CCL-185). The cells were plated in a T25 cell culture flask (Corning). Four milliliters of Kaighn's modification of Ham's F-12 medium (F-12K medium, ATCC) supplemented with 10% fetal bovine serum was added to the flask. The flask was put in a cell culture oven (37 °C, 5% CO_2). The cells were subcultured every 2–3 days at a ratio of 1:3. For subculturing, the cell suspension solution was transferred to

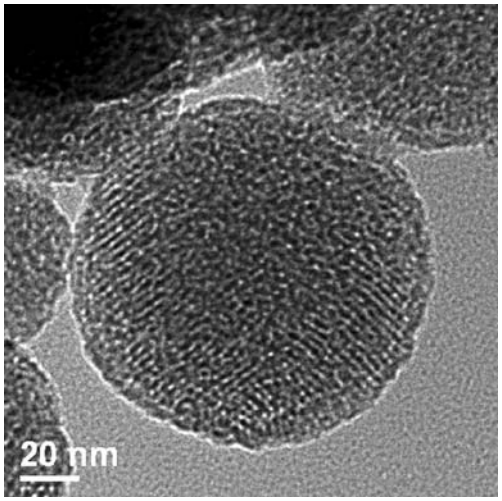

Fig. 1 Transmission electron microscopy image of the mesoporous silica nanoparticles (MSNs) used in our experiments. The MSNs were labeled with fluorescein isothiocyanate and functionalized by tri (ethylene glycol) organic linker. The average size of the MSNs was around 100 nm

a 22 mm×22 mm no.1 poly(L-lysine)-coated cover slip, which was then put into a Petri dish (50 mm×12 mm, Corning). After 1 h, a proper amount of cell growth medium was added to immerse the whole cover slip. Finally, the Petri dish was put back in the cell culture oven for 24 h.

Sample preparation for DIC microscopy

Figure 2 shows a schematic diagram of the experimental setup. Two pieces of double-sided tape were stuck parallel on the top of a precleaned glass slide. The distance between the two pieces of tape was about 15 mm. A cover slip was taken out from the Petri dish, which was prepared in the last step, and the side without cells was cleaned and dried with a Kimwipe. The cover slip was placed carefully on the top of the tapes, with the poly(L-lysine)-coated side facing the glass slide. Then 20 μl MSN suspension solution (30 μg/ml F-12K medium without fetal bovine serum, sonicated for 30 min before use) was added to the chamber formed between the glass slide and the cover slip. The other two open edges of the chamber were sealed by nail polish to prevent evaporation. This sample slide was placed on the stage of the DIC microscope for observation. Because the cells were hung on the ceiling of the chamber, the endocytosed MSN actually moved up from the bottom of the cell against the direction of gravity.

It is crucial to keep the cells alive during the recording period. In our observation, when the cell was dying, the cell membrane would lyse. The cell could no longer stretch out on the cover slip and cell cytoplasm material would flow from the cell. None of these phenomena were observed while the endocytosis event was recorded. In addition, the intracellular organelles, such as granules and mitochondria, were moving around freely. All these observations confirmed that the cells were still alive even after the recording had been completed.

DIC microscopy

An upright Nikon Eclipse 80i microscope equipped with a DIC slider was used for investigations. A ×100 objective lens (Nikon Plan Apo/1.40 oil) was used. The fine-focusing adjustment of the microscope is 0.1 mm per rotation (360°). A motorized rotary stage from Sigma Koki (model no. SGSP-60YAM) was coupled to the fine-adjustment knob on the microscope. The motor was controlled by Intelligent Driver, CSG-602R (Sigma Koki). The travel for each pulse was 0.0025° (0.69 nm). A CCD camera (Cool SNAP ES, Photometrics, Tucson, AZ, USA; pixel size 6.4 μm) was mounted on the microscope. The CCD exposure time was 200 ms at 20-MHz digitization speed unless otherwise specified. Winview32 (Roper Scientific, Princeton, NJ, USA) was used for cell image collection and data processing.

We first distinguished the MSNs from cellular organelles of similar size and shape by fluorescence microscopy using a typical FITC filter set. The microscope can be switched between DIC and fluorescence modes easily. When we observed A549 cells in fluorescence microscopy (control experiment), we did not see fluorescence coming from the other cellular organelles. After we had confirmed the locations of the MSN particles by their fluorescence, we switched the microscope to DIC mode to track their movements. The tracking was accomplished by manually adjusting the focus to the same plane as the MSN. At the same time, vertical sectioning through the entire cell was performed every 5–10 min or when a change in the MSN's vertical position (as indicated by the change in focal plane) was noticed.

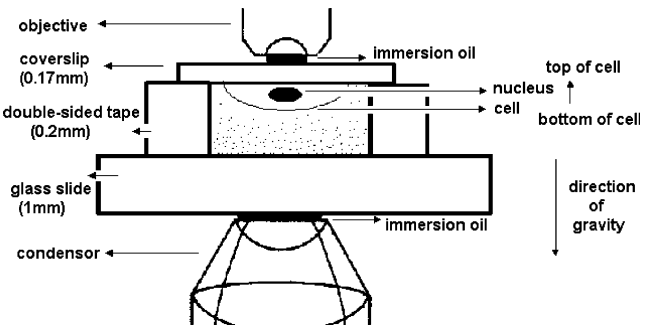

Fig. 2 The experimental setup. Cells (only one cell is shown) grew on a poly(L-lysine)-coated cover slip (0.17 mm). A chamber was made by connecting the glass slide and the cover slip with double-sided tape (0.2 mm). The cell culture medium containing the MSN was added to the chamber. During the process of endocytosis, the MSN diffused from the bottom of the chamber towards the top, against the direction of gravity. Note that the components in this figure are not drawn proportionally

Results and discussion

Generally speaking, to carry out endocytosis, the invaginations or pits of the cell membrane form vesicles which contain foreign materials, and then these vesicles pinch off from the cell membrane, move into the cytosol, and travel towards their final destinations [17]. MSNs are endocytosed by the cell in a similar manner. The whole endocytosis process of a single MSN was recorded by DIC microscopy. To characterize the locations of the MSN and the stages of the endocytosis process, three physical observables were recorded: motion speed, shape, and vertical position.

Motion speed

During the whole process of endocytosis, the MSN, a hard spherical particle with pores, went through three kinds of environment: cell growth medium, cell membrane surface, and cell cytoplasm. They were also the three main stages of endocytosis. The MSN had different motion speeds in each stage.

In the first stage, the MSN underwent significant Brownian motion in the cell growth medium. To have a more quantitative description of the motion, we calculated the diffusion coefficient (D) in two dimensions. The lateral displacements (r) of the MSN between two successive steps were calculated by reading the x–y coordinates of the MSN in a trajectory. The time interval (t) between the two successive steps was 0.2 s. The distribution of lateral displacement is shown in Fig. 3a.

The probability density that a particle diffuses a distance r in a constant time interval t can be expressed by Eq. 1 [18]:

$$P(r)\mathrm{d}r = \frac{2r\mathrm{d}r}{\langle r^2\rangle}\exp\left(-\frac{\rho^2}{\langle r^2\rangle}\right), \quad (1)$$

where $\langle r^2\rangle$, the mean-square displacement, is equal to $4Dt$. Note that the probability $P(r)$ is interchangeable with the number of counts used as the y-axis in Fig. 3, where the total number of measurements was known. Naturally, a large number of displacement measurements—usually generated by Monte Carlo simulation [18]—are required to have a good fit with Eq. 1. Owing to the relatively small sample size from actual experiments, the mean lateral displacement ($\langle r\rangle$) was estimated to be 7.6×10^{-5} cm by fitting the histogram with a typical Gaussian function instead of Eq. 1. Then by using the formula $\langle r^2\rangle=4Dt$ with t=0.2 s, we calculated the diffusion coefficient D to be 2.9×10^{-8} cm^2 s^{-1}.

In order to confirm whether this observed diffusion coefficient had the right order of magnitude, a theoretical diffusion coefficient D* was calculated from the Stokes–Einstein equation:

$$D* = \frac{k_B T}{3\pi\eta d}, \quad (2)$$

where k_B is the Boltzmann constant, T is temperature (295 K), η is the viscosity of the cell growth medium (0.98 cP, Material Safety Data Sheet of F-12K medium, Invitrogen, Carlsbad, CA, USA), and d is the particle diameter (100 nm). The value of D* is 4.4×10^{-8} cm^2 s^{-1}, so D and D* are indeed on the same order of magnitude.

Before the MSN settled down (against gravity) on the cell membrane, it came very close to but not on the cell membrane and still moved rapidly outside the cell. The diffusion coefficient in this intermediate stage was 1.0×10^{-9} cm^2 s^{-1} (Fig. 3b), which was 1 order of magnitude smaller than the diffusion coefficient in the first stage. It is

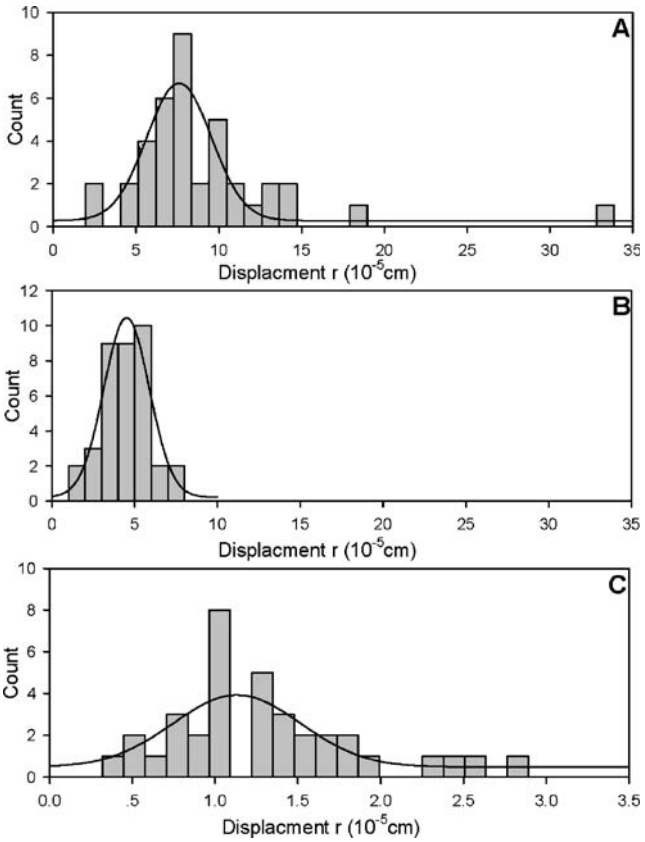

Fig. 3 Histograms of lateral displacement of the MSN at three different stages of endocytosis. The x-axis is the lateral displacement r between two successive steps (time interval 0.2 s) in the trajectory of the MSN, and the y-axis is the number of points that fall in a certain range of lateral displacements. Each histogram was fitted with a Gaussian function to estimate the mean lateral displacement. **a** Unrestricted Brownian motion in the cell growth medium. **b** Restricted Brownian motion near the cell membrane. **c** Restricted Brownian motion inside the cell. The mean lateral displacements were 7.6×10^{-5}, 4.5×10^{-5}, and 11.3×10^{-6} cm for **a**–**c**, respectively. Note that **a** and **b** have an identical scale on the x-axis, but **c** has a scale that is 1 order of magnitude smaller

believed that the attractive force between the ligands on the MSN surface and the corresponding receptors on the cell membrane surface limited Brownian motion of the MSN. When the force was strong enough, the MSN was finally trapped on the cell membrane surface. The MSN eventually crossed the cell membrane (usually less than 10 nm in thickness [19]) to get inside the cell. This was the second stage.

After the MSN had got inside the cell, as evidenced by its vertical location, vide infra, it resumed motion in the cytoplasm, but at a much lower speed than in the first stage. This was the third stage. By using the same method mentioned before, we plotted the lateral displacement distribution shown in Fig. 3c. The diffusion coefficient calculated was 6.4×10^{-10} cm^2 s^{-1}, 2 orders of magnitude smaller than the diffusion coefficient in the first stage. This cannot be explained solely from the viscosity difference between the cell cytoplasm and the cell growth medium, because the aqueous-phase viscosity of the cell cytoplasm is only slightly larger than the viscosity of water (1 cP) [20,

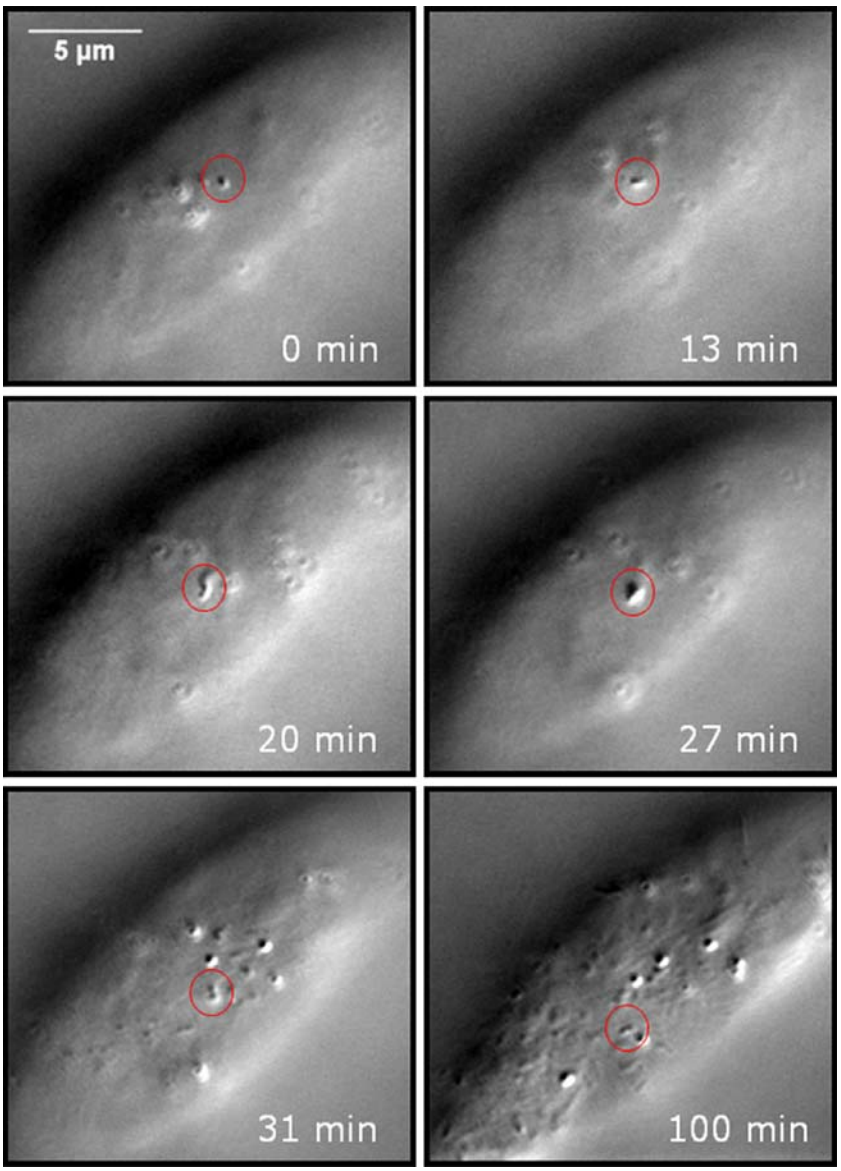

Fig. 4 Endocytosis of a MSN into a living human lung cancer cell. These images show part of the cell, and the large spindle-shaped object is the nucleus. In these images, the MSNs were always in the focal plane of the differential interference contrast microscope. At the beginning (0 min), the MSN was trapped on the cell membrane, and most of the intracellular cell features were out of focus. The shape of the MSN changed several times during this process. Most notably, a large vesicle (endosome) was seen at 27 min. After the MSN had gone inside the cell, as judged by its vertical position, many cell features were on the same horizontal plane as the MSN and could be seen as being in good focus (31 and 100 min)

21]. For example, the cell cytoplasm viscosity of a Chinese hamster ovary cell (an epithelial cell) is 1.0–1.4 cP [20]; therefore, we can assume that an A549 cell, which is also an epithelial cell, has a similar cytoplasmic viscosity. This large difference in diffusion coefficients can be attributed to other properties of cell cytoplasm. It is well known that the cell cytoplasm is not just a homogenous salt buffer solution containing proteins; instead, it has mesh-like networks composed of a small cytoskeleton. The cytoskeleton consists of microtubules (25 nm in diameter), microfilaments (4–6 nm in diameter), and intermediate filaments (7–11 nm in diameter) [22, 23]. These are all too small to be resolved by DIC microscopy. Cytoskeleton dense networks can function as physical obstacles to limit the free diffusion of macromolecules inside the cytoplasm [24]. The reported mesh size in cytoskeleton networks was 20–40 nm [24] or on the order of 100 nm [25]. Considering that the MSN used in our experiment had a diameter of 100 nm, it is reasonable to assume that motion of the MSN inside the cytoplasm was greatly constrained. Besides, cell cytoskeleton is well known for its function in transportation inside the cell [26]. Although there is no report about the requirement of microtubules or small filaments for transportation of a MSN inside the cell, we cannot exclude the possibility. If the MSN was bound to the cytoskeleton and was selectively directed to some subcellular domains along microtubules or filaments, its motion could no longer be described by free-space Brownian motion.

Shape change

The video recorded by DIC microscopy clearly showed that the MSN was enveloped by a vesicle and engulfed into the cell. There were obvious shape changes around the MSN during the process of endocytosis. As shown in Fig. 4, after it had been trapped on the cell membrane, the MSN diffused laterally in the first 15 min, and the shape around the MSN did not change noticeably. In the next 15 min, the volume of the MSN-containing body increased significantly, indicating that the cell had formed a vesicle (endosome) to engulf the MSN. From that time on, the MSN continued to go further inside the cell, and the volume of the MSN-containing vesicle decreased. Further investigation may be needed to distinguish the MSN itself from the vesicle.

Vertical position

In the recorded endocytosis event, the MSN was first trapped on the membrane near the bottom of the cell. Then the MSN moved up and got further inside the cell. This direction of motion was against gravity, which helped to prove that the MSN got inside the cell by endocytosis instead of simply settling onto the cell. The vertical positions of the MSN were measured through optical sectioning accomplished by coupling the DIC microscope with a motorized stage [12]. The vertical position of the MSN is plotted against the recording time in Fig. 5. The MSN traveled about 1.2 μm from the cell membrane towards the nucleus, while the thickness of the entire cell was about 6 μm.

Shape changes (Fig. 4) and vertical position changes (Fig. 5) can be correlated to provide definitive information. In the first 15 min, the position and shape of the MSN did not change significantly, meaning the MSN was still on the cell membrane surface. The granules inside the cell were out of focus because they were not at the same plane as the MSN. From then until 31 min, there were steep changes in vertical position, indicating that the MSN crossed the cell membrane to get inside. This change coincided with the shape change at 20, 27, and 31 min. The volume of the MSN-containing vesicle first increased and then decreased later in this period. After the particle had been internalized, the MSN moved randomly in the three-dimensional space between the cell membrane and the nucleus. At the end of endocytosis (100 min), most granules and other features inside the cell could be seen clearly as they were now at roughly the same focal plane as the MSN.

Conclusion

In this paper we have demonstrated that DIC microscopy can be used to study the endocytosis of a single MSN into a living human lung cancer (A549) cell. The movement of the MSN was observed directly and continuously without staining the cell. The process of endocytosis was characterized by the motion speed, the shape, and the vertical

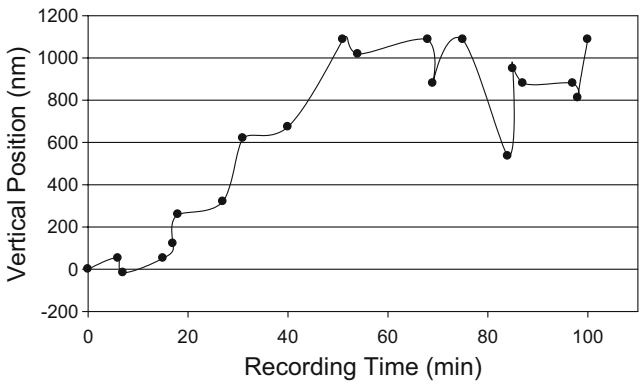

Fig. 5 The vertical position versus the recording time. The difference between the highest and the lowest vertical distances was approximately 1.2 μm. At time 0, the MSN was trapped on the cell membrane and its vertical position was 0. As the endocytosis process continued, the MSN moved deeper into the cell. After roughly 31 min, the MSN moved around inside the cell and its vertical position fluctuated in the range shown. The total thickness of cell was around 6 μm

position of the MSN. By comparing the diffusion coefficients of the MSN inside and outside the cell, we confirmed that the cell cytoplasm was not just a homogeneous viscous solution. The cytoskeleton inside the cytoplasm had a big effect on free diffusion of the MSN inside the cell. Since our DIC microscope had a shallow depth of focus, the accurate vertical position change of the MSN can be measured by optical sectioning. It revealed the three-dimensional distribution of the MSN inside the cell and helped to demonstrate the endocytosis of the MSN. MSNs can be a good drug delivery vector and have lots of applications in controlled drug release systems, as they may be selectively targeted to specific cellular organelles through surface modification. Therefore, drugs can be protected from enzymatic digestion in the cell cytoplasm by capping the channels in MSNs. This approach can be employed to study real-time drug release events in living cells when MSNs or other nanoparticles are used as drug delivery vectors.

Acknowledgements We thank Bob Doyle for valuable discussion. E.S.Y. thanks the Robert Allen Wright Endowment for Excellence for support. The Ames Laboratory is operated for the US Department of Energy by Iowa State University under Contract No. DE-AC02–07CH11358. This work was supported by the Director of Science, Office of Basic Energy Sciences, Division of Chemical Sciences.

References

1. Giri S, Trewyn BG, Stellmaker MP, Lin VSY (2005) Angew Chem Int Ed 44(32):5038–5044
2. Mal NK, Fujiwara M, Tanaka Y (2003) Nature 421(6921):350
3. Park C, Oh K, Lee SC, Kim C (2007) Angew Chem Int Ed 46(9): 1455–1457
4. Moghimi SM, Rajabi-Siahboomi AR (2000) Adv Drug Delivery Rev 41(2):129–133
5. Stein A, Melde BJ, Schroden RC (2000) Adv Mater 12(19): 1403–1419
6. Lu J, Liong M, Zink JI, Tamanoi F (2007) Small 3(8):1341–1346
7. Torney F, Trewyn BG, Lin VSY, Wang K (2007) Nat Nanotechnol 2(5):295–300
8. Slowing II, Trewyn BG, Lin VSY (2007) J Am Chem Soc 129(28):8845–8849
9. Lin YS, Tsai CP, Huang HS, Kuo CT, Huang Y, Huang DM, Chen YC, Mon CY (2005) Chem Mater 17(18):4570–4573
10. Radu DR, Lai CY, Jeftinija K, Rowe EW, Jeftinija S, Lin VSY (2004) J Am Chem Soc 126(41):13216–13217
11. Slowing I, Trewyn BG, Lin VSY (2006) J Am Chem Soc 128(46):14792–14793
12. Li HW, McCloskey M, He Y, Yeung ES (2007) Anal Bioanal Chem 387(1):63–69
13. Salmon ED, Tran P (2007) In: Digital microscopy, 3rd edn. Elsevier, San Diego, pp 335–364
14. Tkachenko AG, Xie H, Liu Y, Coleman D, Ryan J, Glomm WR, Shipton MK, Franzen S, Feldheim DL (2004) Bioconjug Chem 15(3):482–490
15. Zheng M, Davidson F, Huang XY (2003) J Am Chem Soc 125(26):7790–7791
16. Kulak A, Hall SR, Mann S (2004) Chem Commun 2004(5):576–577
17. Mellman I (1996) Annu Rev Cell Dev Biol 12:575–625
18. Saxton MJ (1993) Biophys J 64(6):1766–1780
19. Curtis H, Barnes SN (1989) Biology, 5th edn. Freeman, New York, p 104
20. Srivastava A, Krishnamoorthy G (1997) Arch Biochem Biophys 340(2):159–167
21. Fushimi K, Verkman AS (1991) J Cell Biol 112(4):719–725
22. Lubyphelps K (1994) Curr Opin Cell Biol 6(1):3–9
23. Blum JJ, Lawler G, Reed M, Shin I (1989) Biophys J 56(5):995–1005
24. Lubyphelps K, Taylor DL, Lanni F (1986) J Cell Biol 102(6): 2015–2022
25. Gershon ND, Porter KR, Trus BL (1985) Proc Natl Acad Sci U S A 82(15):5030–5034
26. Radtke K, Dohner K, Sodeik B (2006) Cell Microbiol 8(3): 387–400